Self-consistent linear analysis of slow cyclotron and Cherenkov instabilities

O. Watanabe,[1] K. Ogura,[1] T. Cho,[2] and Md. R. Amin[3]

[1]*Graduate School of Science and Technology, Niigata University, Niigata 950-2181, Japan*
[2]*Plasma Research Center, University of Tsukuba, Tsukuba 305-0006, Japan*
[3]*Bangladesh Institute of Technology, Rajshahi, Bangladesh*

Slow cyclotron and Cherenkov instabilities are analyzed self-consistently for unbounded and cylindrical slow wave systems considering electron beam propagating along the direction of a guiding magnetic field. There are two electromagnetic modes present in the beam that are self-consistent solutions of Maxwell's equations. The wave equation in the beam becomes the Altar–Appelton–Hartree equation in the limit of zero beam velocity. For the unbounded system, the beam couples with the electromagnetic modes corresponding to the X and O modes, resulting in the slow cyclotron and Cherenkov instabilities, respectively. For the cylindrical system, axisymmetric electromagnetic modes in the beam are obtained by superposing the plane normal modes of the unbounded system. Since self-consistent boundary conditions require all field components, axisymmetric electromagnetic modes of cylindrical system are hybrid modes, which are classified as axisymmetric EH and HE modes. The slow cyclotron and Cherenkov instabilities occur for both axisymmetric modes. The temporal growth rate is calculated for each of the instabilities and compared.

I. INTRODUCTION

For an electron beam propagating along the direction of an axial magnetic field, there exist four beam modes, namely, slow and fast space-charge modes and slow and fast cyclotron modes. When the phase velocity of normal electromagnetic (EM) mode is reduced to the beam velocity by means of slow wave structures (SWSs) such as a dielectric loaded waveguide or a periodically modulated waveguide, the microwave radiation can occur at frequencies approximately given by intersections between the slow beam modes and the normal EM mode. Figure 1 shows a dispersion diagram for a dielectric SWS. The slow space-charge and slow cyclotron modes couple with the normal EM modes at the points C and A, respectively. In this paper instabilities at the points C and A are referred to respectively, as ''Cherenkov instability'' and ''slow cyclotron instability.''

The operation of Cherenkov devices like backward wave oscillators (BWOs) and traveling wave tubes (TWTs) are based on the Cherenkov instability and have been studied extensively as a family for powerful slow wave microwave sources [1]. In these devices, a magnetic field is applied to confine an intense electron beam. If the magnetic field is strong enough, it does not affect the stimulated Cherenkov radiation except for cyclotron resonance regimes. Near cyclotron resonance, the output power may decrease [2,3] or increase [4–6] depending on the experimental conditions.

An alternative slow wave high-power microwave source is a slow wave electron cyclotron maser (ECM) based on the slow cyclotron instability [7–11]. In the slow wave ECM, the slow cyclotron and Cherenkov instabilities may compete [10] or cooperate [11] with each other and must be controlled carefully to obtain meaningful oscillation. In Ref. [11], a high power slow wave ECM based on the combined resonance of the slow cyclotron and Cherenkov instabilities has been demonstrated experimentally.

In the previous analyses of Cherenkov devices [12–14],

only longitudinal beam perturbations are considered in order to simplify the analysis. For BWO near the cyclotron resonance or slow wave ECM, vertical perturbations of the beam play an important role and should be taken into account self-consistently. A self-consistent dispersion relation has been derived for an unbounded dielectric system in Ref. [8]. However, the beam interactions were analyzed with an assumption of sufficiently small beam density. Hence, the beam coupled with only one EM mode. It is shown in this paper that there are two normal EM modes and that one couples with the slow space-charge beam mode and the other couples with the slow cyclotron beam mode.

A self-consistent relativistic field theory for the Cherenkov instability has been presented in Refs. [15] and [16] using helix TWT amplifier configurations. In Ref. [15], it has been pointed out for the first time that the wave equation in the beam becomes the Altar–Appelton–Hartree equation [17] in the limit of zero beam velocity. And then, two possible EM modes have been identified and are designated as X and O modes. For convenience, in this paper, the same no-
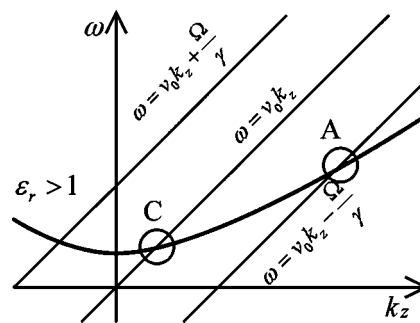

FIG. 1. Dispersion diagram for a dielectric SWS system with $\varepsilon_r > 1$. Points C and A are the intersections of the space-charge mode ($\omega = k_z v_0$) and the slow cyclotron mode ($\omega = k_z v_0 - \Omega/\gamma$) with normal EM modes, respectively. For simplicity, beam charge effects are neglected assuming infinitesimal beam density.

tations are used for the aforementioned modes. There are few self-consistent studies of the slow cyclotron instability in bounded systems. In Ref. [18], the slow cyclotron as well as Cherenkov instabilities in a BWO configuration have been analyzed, taking into account of the beam perturbation perpendicular to the magnetic field. However, an axisymmetric TM mode has been assumed, which is not self-consistent solution of Maxwell's equations in the magnetized electron beam.

This paper is aimed at self-consistent analyses of the slow cyclotron and Cherenkov instabilities. Basic physics of the beam interactions with normal EM modes are examined using a simplified unbounded SWS system. In most of the high power slow wave devices, cylindrical systems are commonly used. In order to clarify a relationship between normal modes of unbounded and cylindrically bounded systems, it is shown that cylindrical normal modes can be derived by superposing plane normal modes in the unbounded system. This relationship has not been pointed out previously in the literatures. A dispersion relation for cylindrical dielectric loaded SWS is derived using cylindrical normal modes. For bounded systems, dispersion equations are derived subject to appropriate boundary conditions. Note that the relationship between the electric polarization and perturbed current density of beam is different from that of rest plasma, since the beam is a moving dielectric medium. Boundary conditions presented in this paper include this fact and are self-consistent. Basic features of the slow cyclotron and Cherenkov instabilities in the physical system are examined by comparing with those for the simplified unbounded system.

The organization of this paper is as follows. In Sec. II, a self-consistent field theory for magnetized electron beams is presented taking into account of three-dimensional perturbed motions of electron in a finite strength magnetic field. A self-consistent dispersion relation for a simplified dielectric system is summarized in Sec. II A. Cylindrical normal modes in the beam are derived by superposing the plane normal modes in Sec. II B. In Sec. III, a self-consistent dispersion relation for a dielectric loaded SWS is presented. Our numerical results are presented in Sec. IV. The slow cyclotron and Cherenkov instabilities are examined for an unbounded dielectric system in Sec. IV A and for a dielectric loaded SWS in Sec. IV B. Discussions and conclusions of this paper are described in Secs. V and VI, respectively.

II. SELF-CONSISTENT FIELDS IN MAGNETIZED ELECTRON BEAM

A. Dispersion relation for an unbounded system

As shown in Fig. 2(a), we consider plane waves in an unbounded dielectric system with a uniform cold electron beam that is neutralized by a fixed ion background and is propagating along a constant magnetic field $\mathbf{B}_0$. The wave vector $\mathbf{k}=(k_{b\perp},0,k_z)$ is in the x-z plane and $\mathbf{B}_0$ in the positive z direction. The initial velocity of the electron is assumed to be $\boldsymbol{\nu}_0=(0,0,\nu_0)$. Beam interactions with EM modes in such a system with arbitrary dielectric constant $\varepsilon_r(>1)$ have been discussed by Case et al. [8], by using a self-consistent linear theory considering three-dimensional beam perturbations.
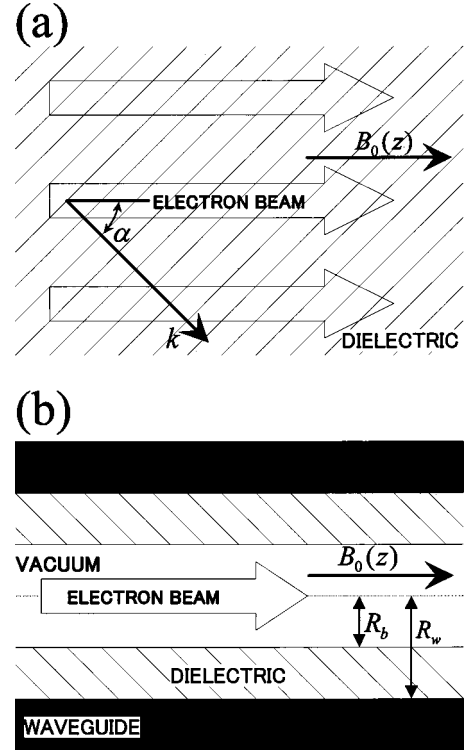

FIG. 2. (a) Unbounded dielectric system with dielectric constant $\varepsilon_r>1$ and (b) cylindrical SWS partially loaded by dielectric ($\varepsilon_r >1$). Finite magnetic field $\mathbf{B}_0$ is applied uniformly in the z direction. An electron beam with monochromatic energy is streaming along the z axis without initial velocity perpendicular to $\mathbf{B}_0$ and is neutralized by a fixed ion background.

Here, we summarize the results for later use. In the following, the subscript 1 is introduced to indicate the first-order perturbed values.

The self-consistent electric field $\mathbf{E}_1^{(\infty)} \exp[i(\mathbf{k}\cdot\mathbf{r}-\omega t)]$ is governed by [8]

$$D^{(\infty)}\cdot\mathbf{E}_1^{(\infty)}=0, \tag{1}$$

where $D^{(\infty)}$ is a 3×3 matrix and its determinant is the dispersion relation, which is given by

$$\varepsilon_r\Gamma^2-\frac{\omega_b^2}{\gamma^3\omega'^2}\Gamma\Gamma_z-\frac{\omega_b^2}{\gamma\omega''^2}\left\{\Gamma\left[k_{b\perp}^2(\varepsilon_r\beta^2-1)+\frac{2\varepsilon_r\omega'^2}{c^2}\right]\right.$$
$$-\frac{\omega_b^2}{\gamma c^2}\left[k_{b\perp}^2(\varepsilon_r\beta^2-1)+\frac{\varepsilon_r\omega'^2}{c^2}+\frac{\Gamma_z}{\gamma^2}+\frac{\Gamma}{\gamma^2}\right]$$
$$\left.+\left(\frac{\omega_b^2}{\gamma^2c^2}\right)^2\right\}=0, \tag{2}$$

where

$$\Gamma=\varepsilon_r\frac{\omega^2}{c^2}-k_{b\perp}^2-k_z^2,$$

$$\Gamma_z=\varepsilon_r\frac{\omega^2}{c^2}-k_z^2. \tag{3}$$

Here, $\omega' = \omega - k_z v_0$, $\omega''^2 = (\omega - k_z v_0)^2 - (\Omega/\gamma)^2$, and $\omega_b^2 = e^2 n_0 / m_0 \varepsilon_0$, where n_0 is the beam electron density, m_0 and $-e$ are, respectively, electron rest mass and charge, where $\Omega = e B_0 / m_0$ is the nonrelativistic cyclotron angular frequency of the electron, and γ is the relativistic factor. Equation (2) can be rewritten as

$$a_4 k_{b\perp}^4 + a_2 k_{b\perp}^2 + a_0 = 0, \tag{4}$$

where

$$a_4 = \varepsilon_r - \frac{\omega_b^2}{\gamma \omega''^2}(1 - \varepsilon_r \beta^2),$$

$$a_2 = -2\Lambda\left(\varepsilon_r - \frac{\omega_b^2}{\gamma^3 \omega'^2}\right) + \frac{\omega_b^2 \Gamma_z}{\gamma^3 \omega'^2 \omega''^2}\left(\frac{\Omega}{\gamma}\right)^2 - \frac{\omega_b^2}{\gamma \omega''^2}$$

$$\times \beta^2(\varepsilon_r - 1)\Gamma_{zb},$$

$$a_0 = \Delta\left(\varepsilon_r - \frac{\omega_b^2}{\gamma^3 \omega'^2}\right),$$

$$\Lambda = \varepsilon_r \frac{\omega^2}{c^2} - k_z^2 - \frac{\omega_b^2}{\gamma c^2}\frac{\omega'^2}{\omega''^2}, \tag{5}$$

$$\Delta = \Lambda^2 - \left(\frac{\omega_b^2}{\gamma c^2}\frac{\omega'}{\omega''^2}\frac{\Omega}{\gamma}\right)^2,$$

$$\Gamma_{zb} = \Gamma_z - \frac{\omega_b^2}{\gamma c^2}.$$

Two values of $k_{b\perp}^2$ can be expressed in terms of ω and k_z as

$$k_{b\perp}^2 = \frac{-a_2}{2a_4} \pm \sqrt{\frac{a_2^2}{4a_4^2} - \frac{a_0}{a_4}}. \tag{6}$$

Two EM modes have the vertical wave number k_+ and k_- corresponding to the $+$ and $-$ signs in Eq. (6), respectively.

In the limit of $v_0 = 0$ with $\varepsilon_r = 1$, Eq. (6) becomes the Altar-Appelton-Hartree equation. With $\omega^2 - \omega_b^2 - \Omega^2 > 0$, k_+^2 and k_-^2 at $k_z = 0$ become

$$k_+^2 = \frac{\omega^2}{c^2}\left(1 - \frac{\omega_b^2}{\omega^2}\right) \quad \text{and}$$

$$k_-^2 = \frac{(\omega^2 - \omega_b^2 + \omega\Omega)(\omega^2 - \omega_b^2 - \omega\Omega)}{c^2(\omega^2 - \omega_b^2 - \Omega^2)}. \tag{7}$$

The former is the O and the latter is the X mode of magnetized electron plasma with a fixed ion background. This correspondence has been pointed out for the first time in the field theory of TWT [15]. In general cases with finite k_z and v_0, $+/-$ signs in Eq. (6) becomes $-/+$ when the sign of the real part of $k_{b\perp}^2 + a_2/2a_4$ changes. For sufficiently large k_z, the EM modes become right and left circular waves. For convenience, we use the same notations as used in Ref. [15], in which the EM mode corresponding to the $O(X)$ mode when $k_z = 0$ and $v_0 = 0$ is designated as the $O(X)$ mode.
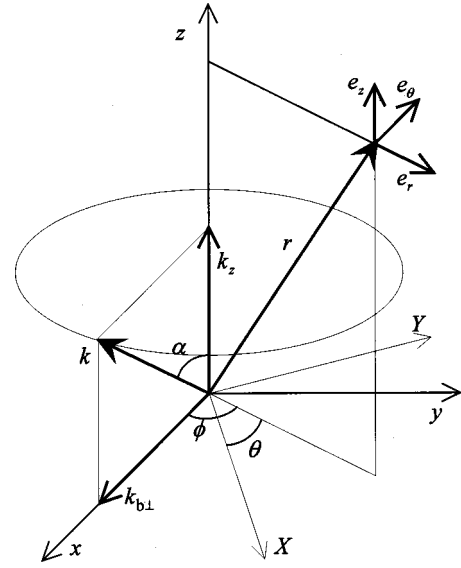

FIG. 3. Rectangular and cylindrical coordinate systems. The X,Y,z axes are fixed and the x,y axes rotate around the z axis so that the conically propagating wave vectors is in the $x-z$ plane. The vectors $\mathbf{e}_r$, $\mathbf{e}_\theta$, and $\mathbf{e}_z$ are the unit vectors in the r, θ, and z directions, respectively.

B. Cylindrical modes in magnetized electron beam

In this section, we consider cylindrical modes in a neutralized beam propagating along a magnetic field in vacuum ($\varepsilon_r = 1$). Axisymmetric normal modes in the beam can be obtained from superposition of the plane O and X modes described in the previous section, which are traveling along the conical paths at an angle $\alpha = \arctan(k_{b\perp}/k_z)$ to the axis [19]. Here, $k_{b\perp} = k_+$ or k_- with $\varepsilon_r = 1$. This is an essentially different point of view from solving Maxwell's equations in a cylindrical coordinate system. The rectangular coordinates (x,y,z) and (X,Y,z) and the cylindrical coordinates (r,θ,z) and (r,ϕ,z) are shown in Fig. 3. Here, the X,Y,z axes are fixed and the x,y axes rotate around the z axis so that the $\boldsymbol{k}$ vector is always in the x-z plane.

By superposing the conically propagating plane waves at a position $r = (r,0,z)$, the axial electric field E_{1z} of the cylindrical wave is given by

$$E_{1z} = \int_0^{2\pi} \mathbf{E}_1^{(\infty)} \cdot \mathbf{e}_z \exp[i(k_{b\perp} r \cos\phi)]d\phi$$

$$= 2\pi E_{1z}^{(\infty)} J_0(k_{b\perp} r). \tag{8}$$

Similarly, electric fields E_{1r} in the r direction and $E_{1\theta}$ in the θ direction are derived as

$$E_{1r} = 2i\pi E_{1x}^{(\infty)} J_1(k_{b\perp} r),$$

$$E_{1\theta} = 2i\pi E_{1y}^{(\infty)} J_1(k_{b\perp} r). \tag{9}$$

Here, we put $\theta = 0$ without loss of generality, the factor $\exp[i(k_z z - \omega t)]$ is suppressed for simplicity, $J_n(k_{b\perp} r)$ is the nth order Bessel function of the first kind and its integral representation [20] is used.

Vertical electric fields, $E_{1x}^{(\infty)}$ and $E_{1y}^{(\infty)}$, are expressed in terms of $E_{1z}^{(\infty)}$ from Eq. (1). Substituting them into Eq. (9), axisymmetric electric-field components can be obtained as

$$E_{1z} = A_{EZ} J_0(k_{b\perp} r),$$

$$E_{1r} = -i \frac{\left(\omega''^2 \Gamma - \frac{\omega_b^2}{\gamma c^2}\omega^2\right)k_z - \frac{\omega_b^2}{\gamma c^2}\omega' \nu_0 \Gamma_b}{(\Lambda k_{b\perp}^2 - \Delta)\omega''^2}$$

$$\times k_{b\perp} J_0'(k_{b\perp} r) A_{EZ},$$

$$E_{1\theta} = \frac{\frac{\omega_b^2}{\gamma c^2}\Pi \frac{\Omega}{\gamma}\omega}{(\Lambda k_{b\perp}^2 - \Delta)\omega''^2} k_{b\perp} J_0'(k_{b\perp} r) A_{EZ}, \qquad (10)$$

where

$$\Gamma_b = \Gamma - \frac{\omega_b^2}{\gamma c^2},$$

$$\qquad (11)$$

$$\Pi = k_z - \frac{\omega \nu_0}{c^2}.$$

Here, $A_{EZ} = 2\pi E_{1z}^{(\infty)}$ and $J_1(\chi) = -dJ_0(\chi)/d\chi$. The first-order magnetic field $\mathbf{B}_1^{(\infty)}$ can be obtained from Faraday's law, $\mathbf{k} \times \mathbf{E}_1^{(\infty)} = \omega \mathbf{B}_1^{(\infty)}$. The Bessel function $J_0(k_{b\perp} r)$ is expressed in terms of the Hankel functions of the first ($H_0^{(1)}$) and second ($H_0^{(2)}$) kinds as $\lfloor H_0^{(1)}(k_{b\perp} r) + H_0^{(2)}(k_{b\perp} r)\rfloor/2$. Since $H_0^{(1)}(k_{b\perp} r)$ and $H_0^{(2)}(k_{b\perp} r)$ represent, respectively, inward and outward propagating waves [19], the cylindrical modes given by Eq. (10) is a standing wave. Its node position is determined by a given boundary.

It is very natural that the wave equation for the cylindrical O and X modes is identical to that for the plane normal modes. The same wave equation and fields are obtained by solving Maxwell's equations in a cylindrical coordinate system [15,21]. When $B_0 \to \infty$, $k_{b\perp}^2$ becomes $\Gamma_z(1 - \omega_b^2/\gamma^3 \omega'^2)$ or Γ_z. The former is the vertical wave number of the TM mode and the latter is that of the TE mode, obtained from the analysis considering only the longitudinal beam perturbation. At $B_0 = 0$, the O and X modes degenerate.

III. AXISYMMETRIC NORMAL MODES FOR A DIELECTRIC LOADED SWS SYSTEM

We consider a dielectric SWS system depicted in Fig. 2(b). An electron beam is a solid cylinder with radius R_b and is neutralized by a fixed ion background. Self-consistent EM modes of the cylindrical SWS are composed of the O and X modes in the beam and TM and TE modes in the dielectric region. The axial components of the perturbed electric and magnetic fields inside the beam ($r \leqq R_b$) may be expressed as

$$E_{1z}^{\text{in}} = A_+ J_0(k_+ r) + A_- J_0(k_- r),$$

$$B_{1z}^{\text{in}} = \frac{i}{c}[B_+ J_0(k_+ r) + B_- J_0(k_- r)],$$

$$B_\pm = \frac{(\omega_b^2/\gamma)\Pi(\Omega/\gamma c)k_\pm^2}{(\Lambda k_\pm^2 - \Delta)\omega''^2} A_\pm, \qquad (12)$$

and outside the beam ($R_W \geqq r \geqq R_b$):

$$E_{1z}^{\text{out}} = D_0 J_0(xr) + E_0 N_0(xr),$$

$$\qquad (13)$$

$$B_{1z}^{\text{out}} = \frac{i}{c}[F_0 J_0(xr) + G_0 N_0(xr)].$$

Here, N_0 is the zeroth-order Bessel function of the second kind, $k_\pm$ are given by Eq. (6) with $\varepsilon_r = 1$, and

$$x^2 = \varepsilon_r \frac{\omega^2}{c^2} - k^2. \qquad (14)$$

For bounded systems, Maxwell's equations should be solved subject to appropriate boundary conditions. At the beam surface ($r = R_b$), we obtain the following four independent equations:

$$E_{1z}^{\text{out}} - E_{1z}^{\text{in}} = 0, \qquad (15a)$$

$$E_{1\theta}^{\text{out}} - E_{1\theta}^{\text{in}} = 0. \qquad (15b)$$

$$B_{1z}^{\text{out}} - B_{1z}^{\text{in}} = -\mu_0 \kappa_{1\theta}, \qquad (15c)$$

$$\varepsilon_r E_{1r}^{\text{out}} - E_{1r}^{\text{in}} = \frac{\sigma_1}{\varepsilon_0}, \qquad (15d)$$

Here, $\kappa_{1\theta}$ is a surface current density in the θ direction and $\sigma_1 = -en_0 r_1$ is a surface charge density given by

$$\sigma_1 = -i\varepsilon_0 \frac{\omega_b^2 \Pi}{\gamma} \sum_{\alpha=+,-} \frac{k_\alpha^2 - \Gamma_{zb}}{(\Lambda k_\alpha^2 - \Delta)\omega''^2} k_\alpha J_0'(k_\alpha R_b) A_\alpha, \qquad (16)$$

where $r_1 = i\nu_1/\omega'$ is a radial displacement of the beam surface. Similar conditions were presented in Ref. [21]. The boundary conditions (15b) and (15d) can be replaced by $B_{1r}^{\text{out}} - B_{1r}^{\text{in}} = 0$ and $B_{1\theta}^{\text{out}} - B_{1\theta}^{\text{in}} = \mu_0 \kappa_{1z}$, respectively. Here, $\kappa_{1z} = \sigma_1 \nu_0$ is a surface current density in the z direction.

Equation (15d) is obtained by applying Gauss's law to the boundary. Note that the beam is a moving dielectric medium. Hence, the electric polarization $\mathbf{P}_1$ and the current density $\mathbf{J}_1$ in Maxwell's equations are given by [22,23]

$$\mathbf{P}_1 = -en_0 \mathbf{r}_1,$$

$$\qquad (17)$$

$$\mathbf{J}_1 = \partial \mathbf{P}_1/\partial t + \nabla \times (\mathbf{P}_1 \times \boldsymbol{\nu}_0).$$

The relationship $\mathbf{J}_1 = \partial \mathbf{P}_1/\partial t$ for a rest dielectric medium is not applicable to moving dielectric medium. Equation (15d) is identical to that for the radial component of electric flux density, which is continuous across the boundary, i.e., the

radial component of electric flux density inside (E_{1r}^{in} $+ \sigma_1/\varepsilon_0$) and outside ($\varepsilon_r, E_{1r}^{out}$) of the beam equal at the boundary.

Since four independent equations obtained at the beam surface contain six unknowns, the normal modes can be characterized by two unknowns, amplitudes $A_\pm$ of the O and X modes. Coefficients of Eq. (13) expressed in terms of $A_\pm$ are

$$D_0 = \frac{1}{Q} \sum_{\alpha=+,-} \left[J_0(k_\alpha R_b)N'_0(xR_b) - \frac{x}{k_\alpha} \right.$$
$$\left. \times \left(1 - \frac{\omega_b^2}{\gamma^3 \omega'^2} \right) J'_0(k_\alpha R_b)N_0(xR_b) \right] A_\alpha,$$

$$E_0 = \frac{1}{Q} \sum_{\alpha=+,-} \left[-J_0(k_\alpha R_b)J'_0(xR_b) + \frac{x}{k_\alpha} \right.$$
$$\left. \times \left(1 - \frac{\omega_b^2}{\gamma^3 \omega'^2} \right) J'_0(k_\alpha R_b)J_0(xR_b) \right] A_\alpha,$$

$$F_0 = \frac{k_\alpha^2}{Q} \frac{(\omega_b^2/\gamma c)(\Omega/\gamma)\Pi}{(\Lambda k_\alpha^2 - \Delta)\omega''^2} \left[J_0(k_\alpha R_b)N'_0(xR_b) \right.$$
$$\left. - \frac{x}{k_\alpha}J'_0(k_\alpha R_b)N_0(xR_b) \right] A_\alpha,$$

$$G_0 = -\frac{k_\alpha^2}{Q} \frac{(\omega_b^2/\gamma c)(\Omega/\gamma)\Pi}{(\Lambda k_\alpha^2 - \Delta)\omega''^2} \left[J_0(k_\alpha R_b)J'_0(xR_b) \right.$$
$$\left. - \frac{x}{k_\alpha}J'_0(k_\alpha R_b)J_0(xR_b) \right] A_\alpha,$$

$$Q = J_0(xR_b)N'_0(xR_b) - J'_0(xR_b)N_0(xR_b). \quad (18)$$

At the wall of $r = R_W$, two electric-field components tangential to the wall, E_{1z} and $E_{1\theta}$, should be zero,

$$E_{1z}(r=R_W) = D_0 J_0(xR_W) + E_0 N_0(xR_W) = 0, \quad (19)$$

$$E_{1\theta}(r=R_W) = \frac{\omega/c}{x}[F_0 J'_0(xR_W) + G_0 N'_0(xR_W)] = 0. \quad (20)$$

From Eqs. (19) and (20), we obtain

$$\begin{bmatrix} P_{z+} & P_{z-} \\ P_{\theta+} & P_{\theta-} \end{bmatrix} \cdot \begin{bmatrix} A_+ \\ A_- \end{bmatrix} = 0. \quad (21)$$

Then, the dispersion relation is

$$P_{z+} \cdot P_{\theta-} - P_{z-} \cdot P_{\theta+} = 0. \quad (22)$$

Here,

$$P_{z\pm} = J_0(k_\pm R_b)[J_0(xR_w)N'_0(xR_b) - J'_0(xR_b)N_0(xR_w)]$$
$$- \frac{x(1-\omega_b^2/\gamma^3\omega'^2)}{\varepsilon_r k_\pm}J'_0(k_\pm R_b)[J_0(xR_w)N_0(xR_b)$$
$$- J_0(xR_b)N_0(xR_w)],$$

$$P_{\theta\pm} = \frac{k_\pm^2 J_0(k_\pm R_b)}{(\Lambda k_\pm^2 - \Delta)\omega''^2}[J'_0(xR_w)N'_0(xR_b)$$
$$- J'_0(xR_b)N'_0(xR_w)] - \frac{k_\pm x J'_0(k_\pm R_b)}{(\Lambda k_\pm^2 - \Delta)\omega''^2}J'_0(k_\pm R_b)$$
$$\times [J'_0(xR_w)N_0(xR_b) - J_0(xR_b)N'_0(xR_w)]. \quad (23)$$

For a waveguide partially filled with an unmagnetized dielectric, it is well known that the normal modes are the TM and TE modes in axisymmetric cases and become hybrid in nonaxisymmetric cases. Hybrid modes are commonly designated as EH and HE, since this designation implies the hybrid nature consisting of the TM and TE modes. Qualitatively, E_z is dominant in the EH mode and H_z is dominant in the HE mode. For the cylindrical system with magnetized electron beam, normal modes are hybrid even in axisymmetric cases. In this paper, axisymmetric hybrid modes are designated as EH_{0n} and HE_{0n}. Here, n is any nonzero integer. The EH_{0n} (HE_{0n}) mode is dominated by TM (TE) component and becomes the TM_{0n} (TE_{0n}) mode in the limit of $B_0 \to \infty$.

IV. NUMERICAL RESULTS

A. Slow cyclotron and Cherenkov instabilities in an infinite system

Figure 4 shows dispersion curves for the infinite dielectric system as depicted in Fig. 2(a) for $B_0 = 0.8$ T. Two EM modes designated as O and X in Sec. II are observed in Fig. 4(a). At $k_z = 0$, the real part of $W4 = k_{b\perp}^2 + a_2/2a_4$ is negative for the O mode and positive for the X mode as shown in Fig. 4(b) and does not change its sign for $0 \le \nu_0 < c$. Hence, the O (X) mode corresponds to the $-$($+$) sign in Eq. (6). With arbitrary k_z and ν_0, the track of the real part of $W4$ is important in determining the EM mode, because the sign in Eq. (6) corresponding to the O and X modes may exchange. In Fig. 4(b), there are four points at which the real part of $W4$ changes the sign, at which the $+/-$ signs in Eq. (6) change. Points of O_1, O_2, and C_1 are attributed to the O mode and X_1 to the X mode. At C_1 and X_1, $W4$ is purely imaginary as can be seen from Fig. 4(c). At O_1 and O_2, a_4 is zero. The frequency at which $a_4 = 0$ corresponds to the upper hybrid frequency for a rest plasma with $\varepsilon_r = 1$. Two fast beam modes interact stably with the EM modes. The slow cyclotron and slow space-charge beam modes couple with the X and O modes, resulting in the slow cyclotron and Cherenkov instabilities, respectively.

At a relatively low B_0, the space-charge mode merges into the slow cyclotron mode as shown in Fig. 5(a). We refer to this instability as ''merged instability.'' Although an isolated Cherenkov instability due to the beam coupling with
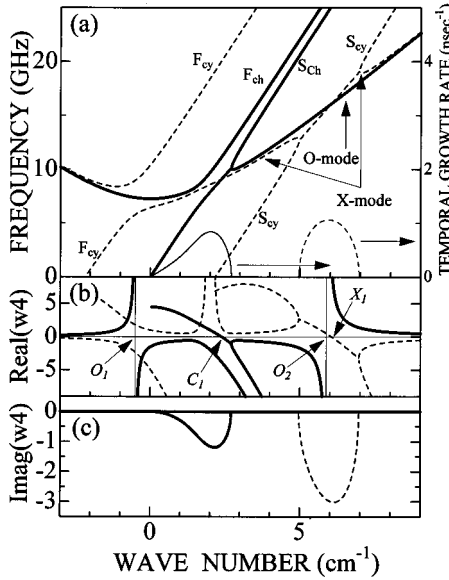
FIG. 4. Dispersion curves for the unbounded dielectric system, (a) real and imaginary parts of frequency $f = \omega/2\pi$ and (b) real and (c) imaginary parts of $W4 = k_{b\perp}^2 + a_2/2a_4$ vs k_z. F_{cy} (S_{cy}) and F_{Ch} (S_{Ch}) indicate the fast (slow) cyclotron and fast (slow) space-charge beam modes. Beam energy and density are 660 keV and 2.6×10^{11} cm^{-3}, respectively, and $\varepsilon_r = 4.0$, $k_{b\perp} = 3.0$ cm^{-1}, and $B_0 = 0.8$ T. At O_1, O_2, C_1, and X_1, the real part of $W4$ changes its sign.

the O mode is observed near $k_z = 2.3$ cm^{-1}, its growth rate is small, about one-fourth of the growth rate of the Cherenkov instability in Fig. 4. The maximum growth rate of the merged instability is determined by the coupling of the X mode with the slow cyclotron mode.
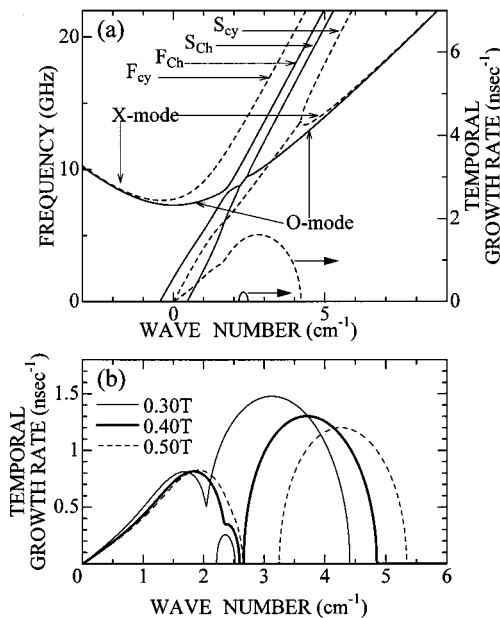

FIG. 5. (a) Dispersion curves for the unbounded dielectric system with $B_0 = 0.25$ T and (b) imaginary part of frequency $f = \omega/2\pi$ for $B_0 = 0.5$, 0.4, and 0.3 T. The parameters other than B_0 are the same as Fig. 4.
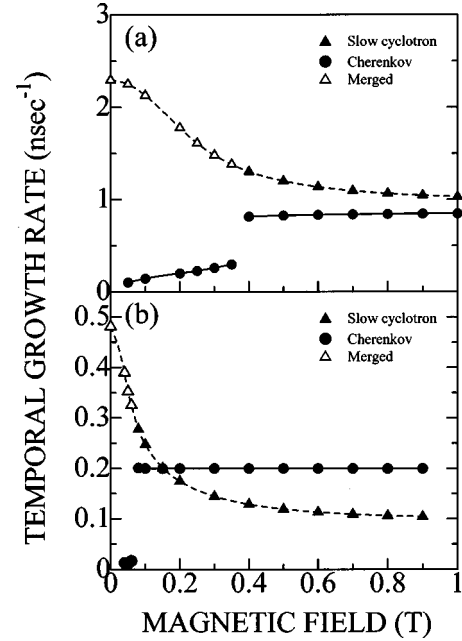

FIG. 6. Maximum temporal growth rates of the Cherenkov, slow cyclotron, and merged instabilities as a function of B_0 for the unbounded system with beam density (a) 2.6×10^{11} cm^{-3} and (b) 2.6×10^{10} cm^{-3}. Beam energy is 660 keV, $\varepsilon_r = 4.0$, and $k_{b\perp} = 3.0$.

In Fig. 5(b), the growth rates near the onset of the merged instability are shown. By decreasing B_0, a bulge appears in the Cherekov instability and becomes the isolated Cherenkov instability. Peak values of these instabilities are depicted as a function of the magnetic field in Fig. 6. Although there are two peaks in the merged instability near its onset as shown in Fig. 5(b), only the largest value is plotted as the "peak value." For $n_0 = 2.6 \times 10^{11}$ cm^{-3} in Fig. 6(a), the growth rate of the slow cyclotron instability is higher than that of the Cherenkov instability and gradually increases with decreasing the magnetic field. The magnetic field has no influence on the Cherenkov instability in the high magnetic field region, where the space-charge and slow cyclotron modes exist separately.

By decreasing the beam density from 2.6×10^{11} to 2.6×10^{10} cm^{-3}, the slow cyclotron instability becomes lower than the Cherenkov instability with $B_0 > 0.15$ T, as shown in Fig. 6(b). However, in the low magnetic field region of $B_0 < 0.1$ T, the slow cyclotron instability becomes higher than the Cherenkov instability. For the merged instability, the maximum value of the growth rate increases with decreasing B_0. The isolated Cherenkov instability is much lower than that of the merged instability and its growth rate decreases gradually with decreasing B_0.

B. Slow cyclotron and Cherenkov instabilities in a dielectric loaded SWS system

Dispersion curves for the dielectric loaded SWS of Fig. 2(b) are shown in Fig. 7. Axisymmetric normal EM modes of EH$_{01}$ and HE$_{01}$ are observed. EH$_{01}$(HE$_{01}$) mode is dominated by the TM (TE) component and is near to TM$_{01}$(TE$_{01}$) mode without the beam. For cylindrical solid beams, there
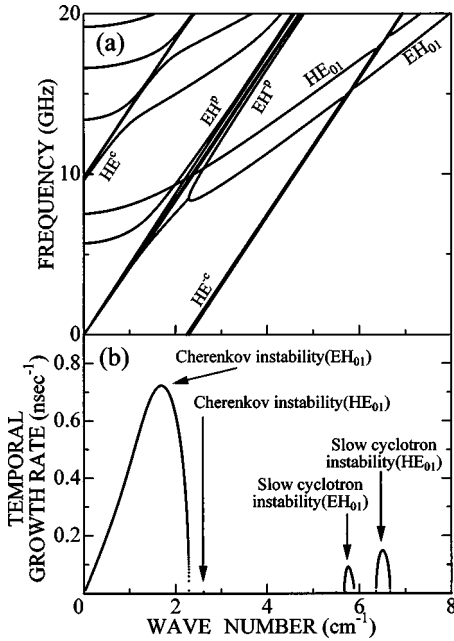
FIG. 7. Dispersion curves of the dielectric loaded SWS shown in Fig. 2(b), (a) real parts of frequency $f = \omega/2\pi$ and (b) imaginary parts of $f = \omega/2\pi$ vs k_z. Parameters of SWS are $R_0 = 14.45$ mm, $R_b = 8.0$ mm, and $\varepsilon_r = 4$ and $B_0 = 0.8$ T. The beam density and energy are respectively, 2.6×10^{11} cm^{-3} and 660 keV that correspond to beam current of 2.3 kA.

are many beam modes that are attributed to multivalued functions J_0 and N_0 in Eq. (13) as reported in Refs. [14] and [18]. Fast space charge and fast cyclotron modes correspond to the Trivelpiece–Gould modes for a rest plasma in a cylindrical pipe [24,25] and are designated EH^p and HE^c modes, respectively. These fast beam modes are stable for the axially streaming electron beam. The slow space-charge and slow cyclotron modes are designated as EH^{-p} and HE^{-c}, respectively. Although the number of beam modes is infinite theoretically, a few dominant modes in the instabilities are plotted in Fig. 7, for simplicity.

The slow cyclotron and Cherenkov instabilities are observed for both EH$_{01}$ and HE$_{01}$ modes. Since axisymmetric normal EM modes consist of the cylindrical O and X modes inside the beam as Eq. (12), EH$_{0n}$ and HE$_{0n}$ modes contain both of them. As a measure of contribution to EH$_{0n}$ and HE$_{0n}$ modes, the O and X components at the beam surface are calculated and compared. For the EH$_{01}$ mode, the O component is four times larger than that the X component in the slow cyclotron instability and increases with decreasing k_z. In the Cherenkov instability, a major component is the O mode and the maximum growth rate of the Cherenkov instability (0.76 ns^{-1}) is much larger than that of the slow cyclotron instability (0.16 ns^{-1}). For the HE$_{01}$ mode, the O and X components are nearly the same in both regions of the Cherenkov and slow cyclotron instabilities. In this case, the growth rate of Cherenkov instability (0.03 ns^{-1}) becomes much smaller than that of the slow cyclotron instability (0.18 ns^{-1}).

Figure 8 shows the magnetic-field dependence of the temporal growth rates of the EH$_{01}$ mode. For the Cherenkov
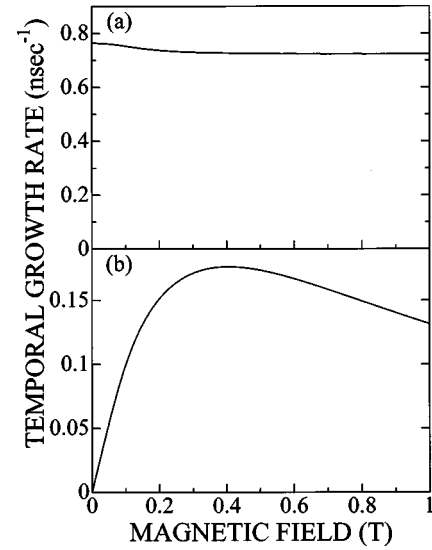

FIG. 8. Maximum temporal growth rates as a function of B_0: (a) the Cherenkov instability and (b) the slow cyclotron instability of the HE$_{01}$ mode. Parameters other than B_0 are the same as in Fig. 7.

instability [Fig. 8(a)], the growth rate is nearly constant with $B_0 > 0.3$ T, and increases slightly with decreasing magnetic field with the relatively low $B_0 < 0.3$ T. The growth rate of the slow cyclotron instability have a maximum value at about $B_0 = 0.4$ T [Fig. 8(b)] and decreases when $B_0 \rightarrow 0$. In contrast to the unbounded case, the slow cyclotron and space-charge beam modes does not merge and the Cherenkov instability is dominant, even in the low magnetic-field region.

V. DISCUSSION

If the Cherenkov and slow cyclotron instabilities are well separated, Eq. (2) with a sufficiently small density of beam may be approximately given by

$$k_{b\perp}^2 = \Gamma_z \quad (X \text{ mode}) \quad \text{and} \quad \Gamma_z + \frac{\omega_b^2}{\varepsilon_r \gamma^3 \omega'^2} \Gamma_z \quad (O \text{ mode})$$
(24)

in the vicinity of the Cherenkov instability and by

$$k_{b\perp}^2 = \Gamma_z + \frac{\omega_b^2}{\gamma \omega''^2 a_4} \left(\varepsilon_r \frac{\omega'^2}{c^2} + \Pi^2 \right) \quad (X \text{ mode}) \quad \text{and}$$

$$\Gamma_z \quad (O \text{ mode})$$
(25)

in the vicinity of the slow cyclotron instability. In this simplification, higher-order terms than ω_b^2 are neglected with the assumption $\omega \gg \omega_b$. Using the same approximation, Eq. (2) was simplified in Ref. [8] as

$$\Gamma \left\{ \varepsilon_r \Gamma - \frac{\omega_b^2}{\gamma^3 \omega'^2} \Gamma_z - \frac{\omega_b^2}{\gamma \omega''^2} \left[k_{b\perp}^2 (\varepsilon_r \beta^2 - 1) + \frac{2\varepsilon_r \omega'^2}{c^2} \right] \right\} = 0.$$
(26)

It is pointed out that Eq. (26) loses O and X mode. The beam couples with only one EM mode, which corresponds to O and X modes of Eqs. (24) and (25), respectively. The other EM mode given by $\Gamma = 0$ is always stable and corresponds to X and O modes of Eqs. (24) and (25), respectively. Equation (26) also loses the isolated Cherenkov instability in the merged region.

The Cherenkov instability includes three modes, the fast and slow space-charge and normal EM modes. The slow cyclotron instability includes two modes, the slow cyclotron and normal EM modes. Considering these characters of interactions, the growth rates are approximately given by

$$\omega_i^C = \frac{\sqrt{3}}{2}\left(\frac{\omega_b^2 c^2 \Gamma_z}{2\varepsilon_r^2 \gamma^3 \omega}\right)^{1/3} \qquad (27)$$

for the Cherenkov instability and by

$$\omega_i^s = \frac{c^2 \omega_b[\varepsilon_r(\omega'^2/c^2) + \Pi^2]^{1/2}}{2\varepsilon_r\sqrt{\omega\Omega}} \qquad (28)$$

for the slow cyclotron instability. Similar growth rates are derived in Ref. [8]. The former is not affected by the magnetic field, while the latter increases with decreasing the magnetic field when $k_{b\perp}$ is real, as shown in Fig. 6. The slow cyclotron instability is more susceptible to n_0 than Cherenkov instability as mentioned in Sec. IV A.

For the slow cyclotron instability, there are two possible mechanisms [8]. In the first mechanism, the force due to $-e\mathbf{v}_0\times\mathbf{B}_1$ converts the original motion in the z direction into the perpendicular plane. The vertical electric field $\mathbf{E}_{1\perp}$ then does work on the electrons, converting the beam mechanical energy into the EM energy. This mechanism is effective to the mode having predominant k_z. In the other mechanism, the cyclotron motions due to the first-order perturbation lead to the beam density bunching. The perturbed beam density and E_{1z} of the EM wave are in phase and can convert the mechanical beam energy to the EM energy. This mechanism is effective to the mode having real $k_{b\perp}$.

For the unbounded system, both mechanisms above are effective in the slow cyclotron instability, which dominates over the Cherenkov instability with the high n_0 or low B_0 as shown in Fig. 6. In the merged instability of the unbounded system, slow cyclotron instability (two modes interaction) suppresses the Cherenkov instability (three modes interaction). For the dielectric loaded SWS system, the normal EM modes coupling with the slow beam modes does not vary its phase along the radial direction, because its radial wavenumber is imaginary. Therefore, in contrast to the unbounded case, the beam density bunching mechanism may not be expected. The slow cyclotron instability in this case is attributed to the $-e\mathbf{v}_0\times\mathbf{B}_1$ mechanism and is much lower than the Cherenkov instability as shown in Figs. 7 and 8. The Cherenkov instability dominates over the slow cyclotron instability even in the low magnetic-field region near $B_0 = 0$.

At $B_0 = 0$, the cyclotron and space-charge beam modes degenerate. The O and X modes also degenerate. For cylindrically bounded systems, axisymmetric TM and TE modes become self-consistent EM modes. The degenerated instability has been investigated for an unbounded dielectric system in Ref. [8] and for a periodic slow wave system in Ref. [18]. This instability is attributed to the beam density bunching mechanism and is a kind of the Cherenkov instability.

VI. CONCLUSIONS

The slow cyclotron and Cherenkov instabilities are analyzed self-consistently for the electron beam propagating along the magnetic field, taking into account of three-dimensional beam perturbations. For the unbounded system, two normal EM modes correspond to the well-known X and O modes of the Altar-Appelton-Hartree equation in a rest plasma and are designated as X and O modes. Cylindrical O and X modes are derived by superposing the plane O and X modes of the unbounded system. Because of this relationship, it is very natural that the wave equation in the beam for the cylindrical system is identical to that for unbounded systems.

For the unbounded system, the X mode couples with the slow cyclotron beam mode and the O mode couples with the slow space-charge beam mode. With relatively large magnetic field, the slow cyclotron and Cherenkov instabilities occur separately. With relatively low magnetic field, the space-charge mode merges into the slow cyclotron mode, resulting in the merged instability. In this instability, the X mode coupling with the slow cyclotron mode is dominant, although a low isolated Cherenkov instability due to the beam coupling with the O mode exists.

For the dielectric loaded SWS system, normal EM modes are hybrid modes having all field components, even in axisymmetric cases. Axisymmetric normal modes are classified into EH_{0n} and HE_{0n} modes, which are dominated by the TM and TE components, respectively. The slow cyclotron and slow space-charge modes are able to couple with EH_{0n} and HE_{0n} modes, which consist of the cylindrical O and X modes inside the beam. Axially streaming electron beam without initial vertical velocity is able to excite EM modes in physical systems at the slow cyclotron resonance as well as at the Cherenkov resonance. In contrast to the unbounded case, the slow cyclotron and space-charge beam modes exist separately, even in the low magnetic-field region. The slow cyclotron instabilities described in this paper may present a promising way of generating microwaves and play an essential role in the slow cyclotron masers driven by an electron beam with predominant axial velocity.

[1] J. N. Benford and J. A. Swegle, *High Power Microwaves* (Artech House, Boston, 1992).

[2] V. S. Ivanov, S. I. Krementsov, V. A. Kutsenko, M. D. Raizer, A. A. Rukhadze, and A. V. Fedotov, Zh. Tekh. Fiz. **51**, 970 (1981) [Sov. Phys. Tech. Phys. **26**, 580 (1981)].

[3] Y. Carmel, W. R. Lou, T. M. Antonsen, Jr., J. Rodgers, B. Levush, W. W. Destler, and V. L. Granatstein, Phys. Fluids B **4**, 2286 (1992).

[4] Yu. V. Tkach, N. P. Gadetskii, Yu. P. Bliokh, E. A. Lemberg, M. G. Lyubarskii, V. V. Ermolenko, V. V. Dyatlova, S. I. Naisteter, I. I. Magda, S. S. Pushkarev, and G. V. Skachek, Fiz. Plazmy **5**, 1012 (1979) [Sov. J. Plasma Phys. **5**, 566 (1979)].

[5] K. Ogura, K. Minami, K. Kurashina, W. S. Kim, T. Watanabe, K. Ishi, and S. Sugito, Fusion Eng. Des. **26**, 365 (1995).

[6] M. R. Amin, K. Minami, K. Ogura, X. Zheng, and T. Watanabe, J. Phys. Soc. Jpn. **64**, 4473 (1995).

[7] A. N. Didenko, A. R. Borisov, G. P. Fomenko, A. S. Shlapakovskii, and Yu. G. Shtein, Pis'ma Zh. Tekh. Fiz. **9**, 1331 (1983) [Sov. Tech. Phys. Lett. **9**, 572 (1983)].

[8] W. B. Case, R. D. Kaplan, J. E. Golub, and J. E. Walsh, J. Appl. Phys. **55**, 2651 (1984).

[9] T. H. Kho and A. T. Lin, Phys. Rev. A **38**, 2883 (1988).

[10] T. H. Kho and A. T. Lin, IEEE Trans. Plasma Sci. **18**, 513 (1990).

[11] K. Ogura, M. R. Amin, K. Minami, X. D. Zheng, Y. Suzuki, W. S. Kim, T. Watanabe, Y. Carmel, and V. L. Granatstein, Phys. Rev. E **53**, 2726 (1996).

[12] N. E. Belov, N. I. Karbushev, A. A. Rukhadze, and S. Yu. Udovichenko, Fiz. Plazmy **9**, 785 (1983) [Sov. J. Plasma Phys. **9**, 454 (1983)].

[13] J. A. Swegle, J. W. Poukey, and G. T. Leifeste, Phys. Fluids **28**, 2882 (1985).

[14] K. Minami, Y. Carmel, V. L. Granatstein, W. W. Destler, W. Lou, D. K. Abe, R. A. Kehs, M. M. Ali, T. Hosolawa, K. Ogura, and T. Watanabe, IEEE Trans. Plasma Sci. **18**, 537 (1990).

[15] H. P. Freund, N. R. Vanderplaats, and M. A. Kodis, IEEE Trans. Plasma Sci. **21**, 654 (1993).

[16] H. P. Freund, E. G. Zaidaman, M. A. Kodis, and N. R. Vanderplaats, IEEE Trans. Plasma Sci. **24**, 895 (1996).

[17] T. H. Stix, *Waves in Plasmas* (AIP, New York, 1992).

[18] K. Ogura, T. Azegami, O. Watanabe, and T. Watanabe, J. Phys. Soc. Jpn. **67**, 3462 (1998).

[19] R. Courant and D. Hirbert, *Methods of Mathematical Physics* (Wiley, New York, 1989), Vol. 2, Chap. 3.

[20] M. Abramowitz and I. A. Stegun, *Handbook of Mathematical Functions* (Dover, New York, 1972).

[21] O. Watanabe and K. Ogura, J. Plasma Fusion Res. **3**, 601 (2000); *Proceedings of the 10th International Toki Conference, Toki, Japan, 2000*, edited by A. Sagara, Y. Hirooka, N. Noda, and O. Motojima (The Japan Society of Plasma Science and Nuclear Fusion Research, Nagoya, 2000).

[22] D. L. Bobroff, IRE Trans. Electron Devices **6**, 68 (1959).

[23] W. K. H. Panofsky and M. Phillips, *Classical Electricity and Magnetism* (Addison-Wesley, Reading, MA, 1962).

[24] A. W. Trivelpiece and R. W. Gould, J. Appl. Phys. **30**, 1784 (1959).

[25] S. T. Ivanov and E. G. Alexov, J. Plasma Phys. **43**, 51 (1990).